

Diffuse lymphoma involvement of the spinal cord showed on [¹⁸F]FDG PET/MRI

Chunyan Zhao*, Liqian Yu*, Lin Li, Minggang Su

Department of Nuclear Medicine, West China Hospital, Sichuan University, Sichuan, China

*These authors contributed equally to this work

[Received: 14 III 2024; Accepted: 12 VI 2024]

Abstract

A 61-year-old woman with diffuse large B-cell lymphoma received a fluorine-18-deoxyglucose positron emission tomography/computed tomography ([¹⁸F]FDG PET/CT) for staging. Because of the obvious uptake of [¹⁸F]FDG in the spinal cord and brain, a positron emission tomography/magnetic resonance imaging (PET/MRI) was performed after the positron emission tomography/computed tomography (PET/CT). The images showed diffuse [¹⁸F]FDG uptake of the spinal cord and increased T2 signal intensity on MRI, which was suspected to be lymphoma involvement. The patient was diagnosed with diffuse large B-cell lymphoma involving the right maxillofacial region, right cervical lymph nodes, cervix, brain and spinal cord (stage IV of non-germinal center B-cell origin). After chemotherapy, the spinal [¹⁸F]FDG uptake level decreased significantly, which was considered to be a partial metabolic response. Our case was different from prior, which indicated the pattern of spinal cord involvement by lymphoma was focal.

KEYwords: lymphoma; central nervous system; spinal cord; PET

Nucl Med Rev 2024; 27: 24–27

Introduction

Lymphoma involvement of the spinal cord is rare [1, 2], and once it occurs the prognosis is poor [3]. Prior reports indicate that the typical pattern of spinal cord involvement by lymphoma was focal [1, 2, 4, 5]. Interestingly, we present a case of lymphoma diffusely invading the spinal cord. In addition, the diagnosis of spinal cord involvement by lymphoma was usually made by MRI, cerebrospinal fluid cytology or nerve root biopsy [4–7]. However, these tests may not provide accurate assessment, or cause nerve root damage [8]. Our case showed PET/MRI might play a role in evaluating spinal cord involvement by lymphoma.

Case presentation

A 61-year-old woman with a tender mass on her right maxillofacial region for more than 2 months was admitted. She also complained about dizziness and memory loss. A biopsy of the maxillofacial mass was performed, and the immunophenotype showed CD45 (–), PCK (–), Des (–), S-100 (–), CD20 (+), CD3 (–), CD30 (–), CD10 (–), BCL-6 (+), MUM-1 (+), BCL-2 (+, > 90%),

C-MYC (+, about 40%), CyclinD1 (–), CD23 (–), TdT (–), CD99 (–), P53 (–), PD-1 (+, about 80%), Ki-67/MIB-1 (+, about 90%), EBER1/2-ISH (–), supporting the diagnosis of diffuse large B-cell lymphoma. Then, a [¹⁸F]FDG PET/CT was performed for staging. Because of the obvious uptake of [¹⁸F]FDG in the spinal cord and brain, a [¹⁸F]FDG PET/MRI was performed after the PET/CT (Fig. 1). Based on the information mentioned above, right maxillofacial lymphoma with cervical node and central nervous involvement was diagnosed.

Subsequently, the patient received a brain contrast MRI. It showed patchy enhancements on the enhanced T1 weighted image (Fig. 2A), which supported the diagnosis of central nervous lymphoma involvement. After 2 cycles of R-BTK plus CHOP (rituximab, obrutinib, cyclophosphamide, vindesine, liposomal doxorubicin, and prednisone) therapy, the patient developed weakness of the right lower limb, slurred speech, and crooked mouth. Therefore, the treatment plan was changed to R-CHOP plus HDMTX (rituximab, cyclophosphamide, vindesine, liposomal doxorubicin, prednisone, methotrexate). Later, the patient developed drug resistance, and brain contrast CT showed progression of brain lesions (Fig. 2B).

Then the regimen was changed into rituximab, lenalidomide, obrutinib and sintilimab. After 2 cycles of treatment, the symptoms were relieved. To assess the response to treatment, a second [¹⁸F]FDG PET/MRI was performed and showed a partial metabolic response of the initial tumor lesions in the right maxillofacial region (Fig. 3A). Partial metabolic response was also observed in the spinal cord (Fig. 3B–D) and intracranial

Correspondence to: Minggang Su, Department of Nuclear Medicine, West China Hospital, Sichuan University, No. 37 Guoxue Alley, Chengdu, Sichuan (610041), PR China
e-mail: suminggang@sina.com; phone: + 86-18980606733;
fax: 862885423818

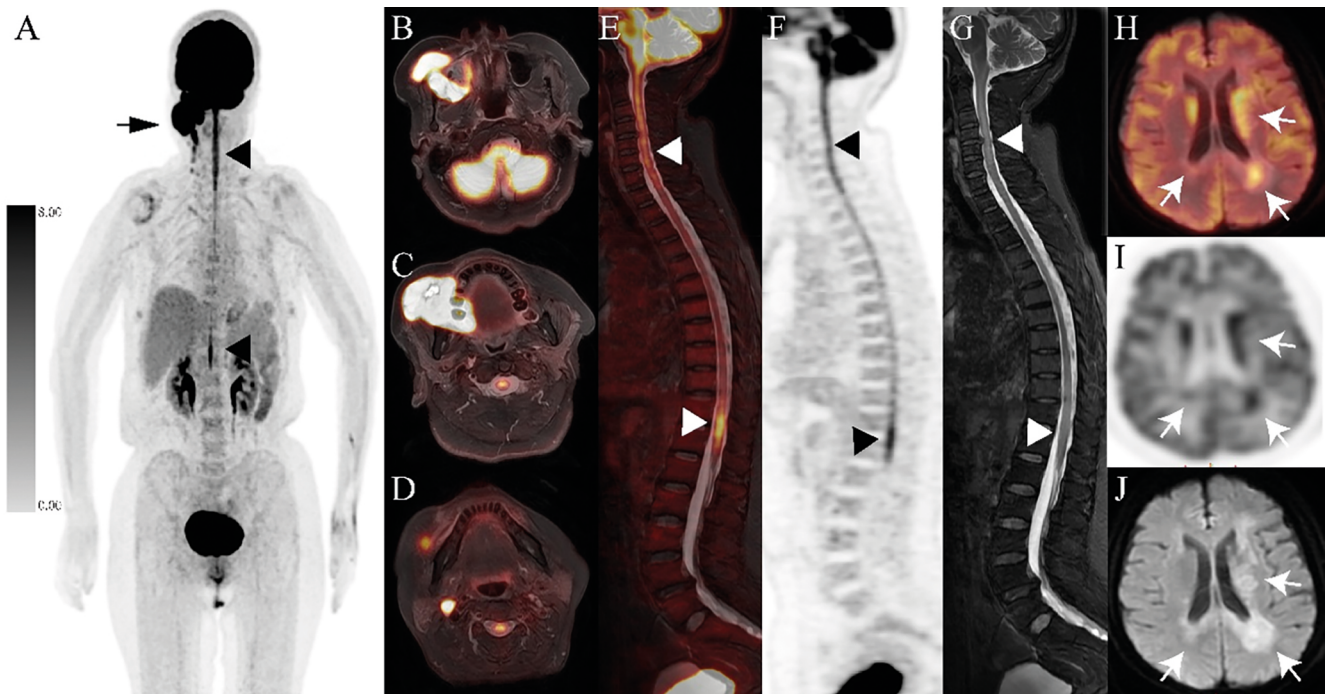


Figure 1. [^{18}F]FDG PET whole-body maximum intensity projection image (A), axial fused [^{18}F]FDG PET/MR images (B–D), sagittal fused [^{18}F]FDG PET/MR image (E), sagittal [^{18}F]FDG PET image (F), sagittal MR T2 weighted image (G), axial fused [^{18}F]FDG PET/MR image (H), axial [^{18}F]FDG PET image (I), axial MR T2 weighted image (J); Multiple foci of increased tracer uptake seen in the right side of maxillofacial region and ipsilateral neck (*black arrow*), and midline (*black arrowheads*) (A); The maxillofacial and cervical foci were located at the known maxillofacial mass and lymphadenopathies with SUV_{max} of 24.6 and 12.3 respectively (B–D); The linear midline uptake was located on the spinal cord diffusely involving the whole cord with a SUV_{max} of 7.7 (*white arrowheads*) (E); (*black arrowheads*) (F); The T2 signal intensity of the spinal cord increased on corresponding MR T2 weighted images (*white arrowheads*) especially the cervical segment (G); Increased [^{18}F]FDG uptake in the bilateral paraventricular white matter with a SUV_{max} of 15.3 was also noticed on axial fusion [^{18}F]FDG PET/MR and PET images (H, I, arrows); Diffuse weighted image showed high signal intensity at the corresponding site (J)

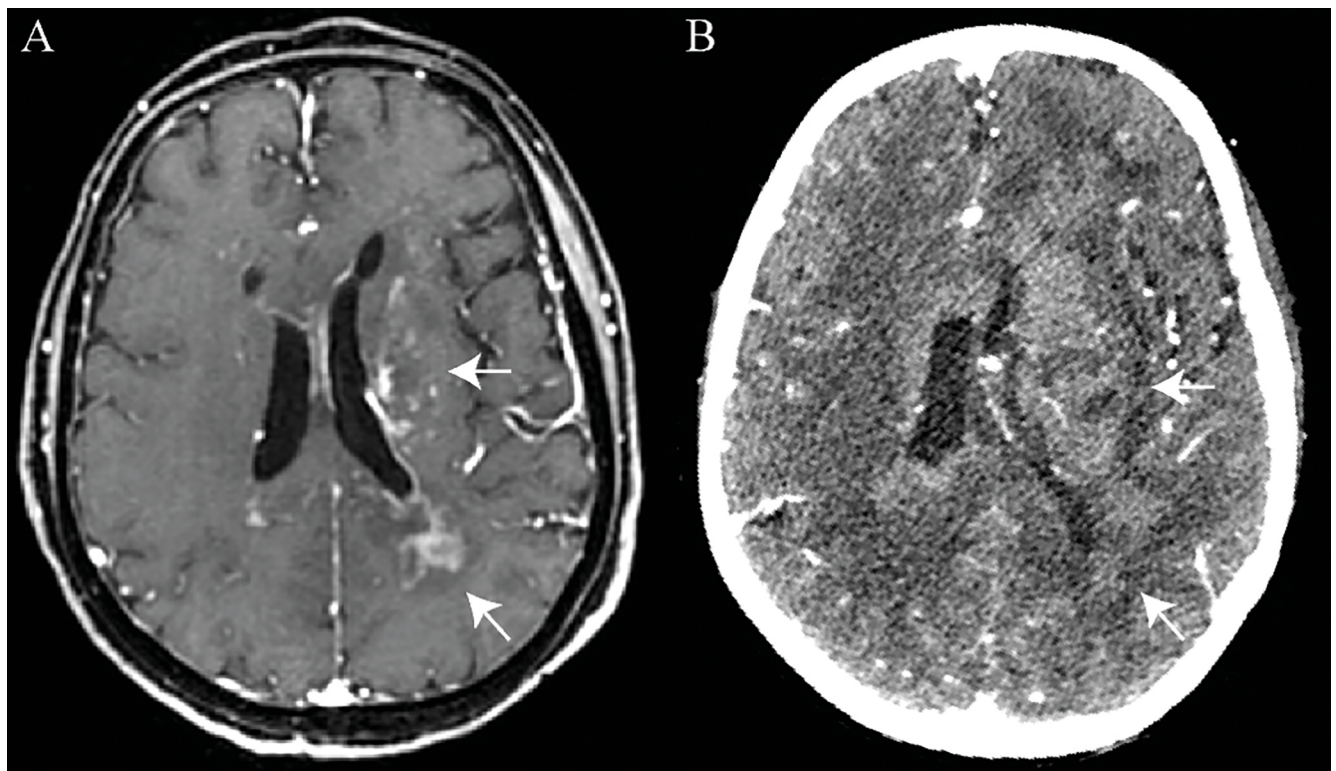


Figure 2. Patchy enhancements on enhanced T1 weighted image in the brain contrast MRI (*arrows*) (A); Brain contrast CT showed progression of brain lesions (*arrows*) (B)

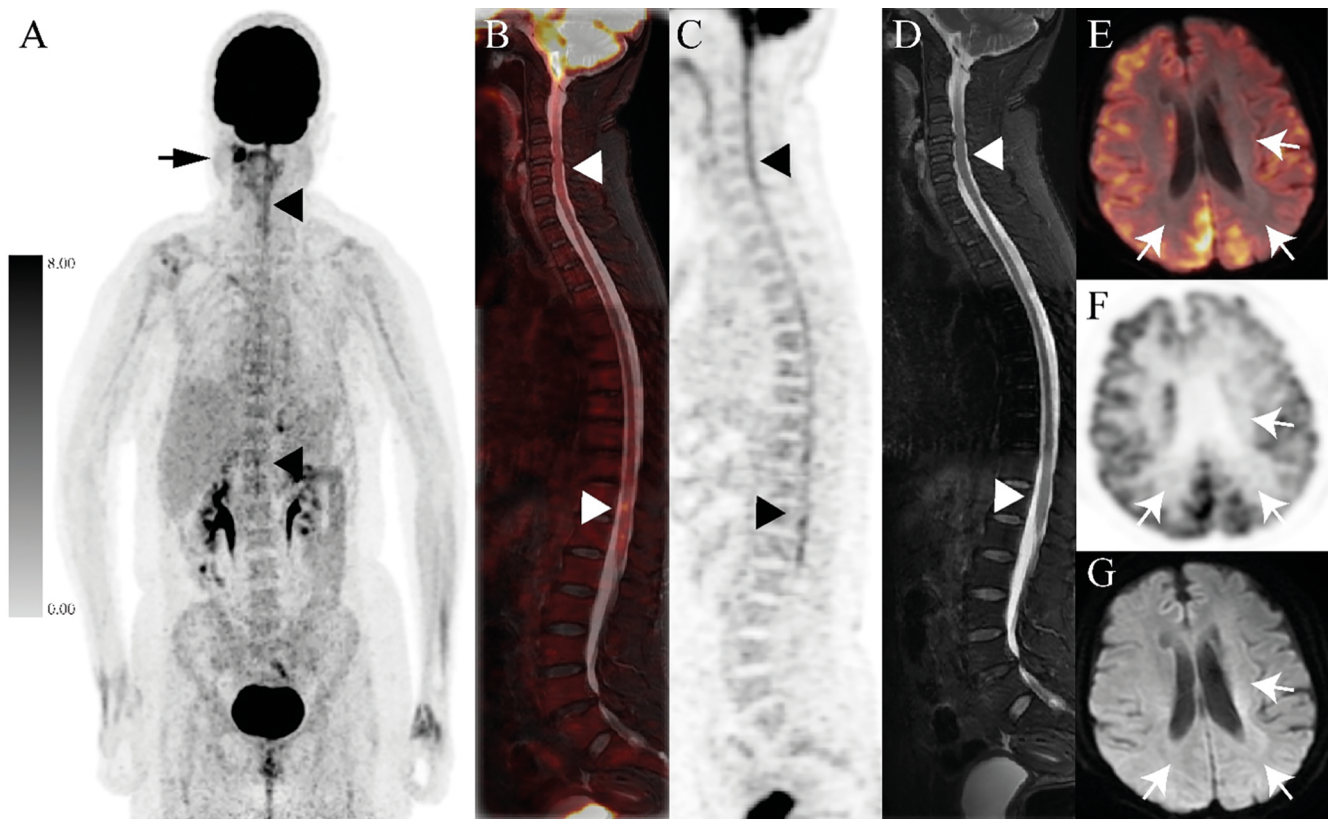


Figure 3. [^{18}F]FDG PET whole-body maximum intensity projection image (A), sagittal fused [^{18}F]FDG PET/MR image (B), sagittal [^{18}F]FDG PET image (C), sagittal MR T2 weighted image (D), axial fused [^{18}F]FDG PET/MR image (E), axial [^{18}F]FDG PET image (F), MR DWI (G); Partial metabolic response of the initial tumor lesions on the right maxillofacial region in the PET MIP image (*black arrow and arrowhead*) (A); Partial metabolic response was also observed in spinal cord (*white arrowhead*) (B); (*black arrowhead*) (C); (*white arrowhead*) (D); and in the bilateral paraventricular white matter (*white arrows*) (E–G)

lesions (Fig. 3E–G). One year later, the patient passed away due to tumor progression.

Differential considerations for this diffuse pattern should include paraneoplastic myelitis, but most often are associated with small cell lung cancer and breast cancer [9]. Paraneoplastic syndrome caused by lymphoma often occurs in the cerebellum [9, 10], and is more common in Hodgkin lymphoma and young men [11]. In addition, it is necessary to distinguish it from the physiological uptake of the spinal cord. Generally, the SUV value of the physiological uptake of the spinal cord is low [12].

Article information and declarations

Acknowledgments

This study was supported by the “1.3.5 project for disciplines of excellence, West China Hospital, Sichuan University (ZYGD18016)”.

Author contributions

Conceptualization — CZ, MS; methodology — CZ, LY, MS; formal analysis and investigation — CZ, LY; writing: original draft preparation — CZ, LY; writing: review and editing — CZ, LY, LL; funding acquisition — LL; resources — MS, LL; supervision — MS.

Conflicts of interest

All authors acknowledge no conflict of interest.

Funding

1.3.5 project for disciplines of excellence, West China Hospital, Sichuan University (ZYGD18016).

Supplementary material

None.

References

- Rao A, Griffiths R, Arnaoutakis K. Paralyzed by a rare cause: an unusual case of metastatic diffuse large B cell lymphoma of the intramedullary spinal cord. *Ann Hematol.* 2014; 93(2): 337–338, doi: [10.1007/s00277-013-1792-3](https://doi.org/10.1007/s00277-013-1792-3), indexed in Pubmed: [23712293](https://pubmed.ncbi.nlm.nih.gov/23712293/).
- Ban Y, Jing Z, Zou J. Multiple secondary cauda equina non-Hodgkin's lymphoma: a case report and literature review. *BMC Cancer.* 2019; 19(1): 594, doi: [10.1186/s12885-019-5800-4](https://doi.org/10.1186/s12885-019-5800-4), indexed in Pubmed: [31208357](https://pubmed.ncbi.nlm.nih.gov/31208357/).
- Fleury I, Amorim S, Mounier N, et al. Management and prognosis of 66 patients with B-cell non-Hodgkin lymphoma presenting with initial spinal cord compression: a French retrospective multicenter study. *Leuk Lymphoma.* 2015; 56(7): 2025–2031, doi: [10.3109/10428194.2014.977884](https://doi.org/10.3109/10428194.2014.977884), indexed in Pubmed: [25347431](https://pubmed.ncbi.nlm.nih.gov/25347431/).

4. Zagami AS, Granot R. Non-Hodgkin's lymphoma involving the cauda equina and ocular cranial nerves: case reports and literature review. *J Clin Neurosci.* 2003; 10(6): 696–699, doi: [10.1016/s0967-5868\(03\)00089-4](https://doi.org/10.1016/s0967-5868(03)00089-4), indexed in Pubmed: [14592623](https://pubmed.ncbi.nlm.nih.gov/14592623/).
5. Broen M, Draak T, Riedl RG, et al. Diffuse large B-cell lymphoma of the cauda equina. *BMJ Case Rep.* 2014; 2014, doi: [10.1136/bcr-2014-205950](https://doi.org/10.1136/bcr-2014-205950), indexed in Pubmed: [25368124](https://pubmed.ncbi.nlm.nih.gov/25368124/).
6. Nishida H, Hori M, Obara K. Primary B-cell lymphoma of the cauda equina, successfully treated with high-dose methotrexate plus high-dose cytarabine: a case report with MRI findings. *Neurol Sci.* 2012; 33(2): 403–407, doi: [10.1007/s10072-011-0752-8](https://doi.org/10.1007/s10072-011-0752-8), indexed in Pubmed: [21898094](https://pubmed.ncbi.nlm.nih.gov/21898094/).
7. Teo MK, Mathieson C, Carruthers R, et al. Cauda equina lymphoma — a rare presentation of primary central nervous system lymphoma: case report and literature review. *Br J Neurosurg.* 2012; 26(6): 868–871, doi: [10.3109/02688697.2012.697225](https://doi.org/10.3109/02688697.2012.697225), indexed in Pubmed: [22768968](https://pubmed.ncbi.nlm.nih.gov/22768968/).
8. Nakajima H, Motomura M, Yamaguchi M, et al. [Leptomeningeal infiltration of primary CNS B-cell lymphoma diagnosed by the biopsy of cauda equina: a case report]. *Rinsho Shinkeigaku.* 2013; 53(10): 803–808, doi: [10.5692/clinicalneuro.53.803](https://doi.org/10.5692/clinicalneuro.53.803), indexed in Pubmed: [24225563](https://pubmed.ncbi.nlm.nih.gov/24225563/).
9. Madhavan AA, Carr CM, Morris PP, et al. Imaging review of paraneoplastic neurologic syndromes. *AJNR Am J Neuroradiol.* 2020; 41(12): 2176–2187, doi: [10.3174/ajnr.A6815](https://doi.org/10.3174/ajnr.A6815), indexed in Pubmed: [33093137](https://pubmed.ncbi.nlm.nih.gov/33093137/).
10. Gheysens O, Deroose CM, Tousseyn T, et al. Hodgkin lymphoma-associated paraneoplastic cerebellar degeneration on FDG-PET/CT. *Br J Haematol.* 2014; 164(4): 468, doi: [10.1111/bjh.12619](https://doi.org/10.1111/bjh.12619), indexed in Pubmed: [24460525](https://pubmed.ncbi.nlm.nih.gov/24460525/).
11. Hammack J, Kotanides H, Rosenblum MK, et al. Paraneoplastic cerebellar degeneration. II. Clinical and immunologic findings in 21 patients with Hodgkin's disease. *Neurology.* 1992; 42(10): 1938–1943, doi: [10.1212/wnl.42.10.1938](https://doi.org/10.1212/wnl.42.10.1938), indexed in Pubmed: [1407576](https://pubmed.ncbi.nlm.nih.gov/1407576/).
12. Aiello M, Alfano V, Salvatore E, et al. [F]FDG uptake of the normal spinal cord in PET/MR imaging: comparison with PET/CT imaging. *EJNMMI Res.* 2020; 10(1): 91, doi: [10.1186/s13550-020-00680-8](https://doi.org/10.1186/s13550-020-00680-8), indexed in Pubmed: [32761394](https://pubmed.ncbi.nlm.nih.gov/32761394/).